Agricultural and Forest Meteorology 256–257 (2018) 207–219

Contents lists available at ScienceDirect

Agricultural and Forest Meteorology

journal homepage: www.elsevier.com/locate/agrformet

Scaling up spring phenology derived from remote sensing images

Dailiang Peng[a], Chaoyang Wu[b,*], Xiaoyang Zhang[c], Le Yu[d,*], Alfredo R. Huete[e], Fumin Wang[f], Shezhou Luo[a], Xinjie Liu[a], Helin Zhang[a]

[a] Key Laboratory of Digital Earth Science, Institute of Remote Sensing and Digital Earth, Chinese Academy of Sciences, Beijing 100094, China
[b] Institute of Geographical Sciences and Natural Resources Research, Chinese Academy of Sciences, Beijing 100101, China
[c] Geospatial Sciences Center of Excellence, South Dakota State University, Brookings, SD 57007, USA
[d] Ministry of Education Key Laboratory for Earth System Modelling, Department of Earth System Science, Tsinghua University, Beijing, 100084, China
[e] Climate Change Cluster (C3), University of Technology Sydney, NSW 2007, Australia
[f] Zhejiang University, Institute of Agricultural Remote Sensing and Information Technology, Hangzhou, 310058, China

ARTICLE INFO

Keywords:
Scale effecting
Scale up
Spring phenology
Validation
Average
Percentile

ABSTRACT

Land surface phenology, especially spring phenology, has been reported as a powerful indicator of ecosystem responses to climate change. It also exerts strong control on the carbon, water and energy balances and, hence, climatic feedbacks. Researchers have produced numerous spring phenology products from various coarse-resolution remote sensing data at regional or global scales. Scaling up observations of spring phenology from plot-level (or finer resolution) to coarser resolution is important for the validation, synthesis, and evaluation of those products. The best method for scaling up is unclear although coarse resolution data can be obtained by averaging across fine-scale pixels, or selecting the start of spring phenology (SOS) date associated with the earliest 30% (or another percentile) of fine-scale pixels within a coarse-scale pixel. In this study, we tested different methods that were average and percentile approaches to aggregate SOS as measured at 250 m (SOS (250 m)) resolution to 8 km (SOS (8 km)) resolution pixels, and then to ecosystems and national scales for the continental United States. The results indicated that the average absolute difference (AAD) between SOS (250 m) and SOS (8 km) from the average approach was close to that achieved by the percentile approach. Relatively large AAD values occurred in the western and southern regions of the continental United States. The distribution of AAD was positively related to landscape heterogeneity. The percentile approach generally yielded smaller AADs than the average approach did, but these two approaches performed similarly. Across landscapes and ecosystems, the optimal percentile usually ranged from 30–45th instead of a single value. Our findings indicated that the percentile approach may be best for finer scale areas, but that the average approach is an adequate alternative for scaling up SOS in most circumstances. In addition, the detailed error distributions of scaling up spring phenology across scales are helpful to identify the appropriate method of scaling up for validating the coarse SOS products derived from remote sensing images.

1. Introduction

Phenology indicates the timing of periodic events in the life cycle of living organism (Piao et al., 2015). Land surface phenology (LSP), especially start of spring phenology (SOS), has been reported as an independent measure and powerful indicator of ecosystem responses to climate change (Linderholm, 2006; White et al., 2009; Zhang et al., 2014; Piao et al., 2015; Peng et al., 2017a,b,c). The trend of earlier spring phenology, particularly at mid- and high-latitudes in the Northern Hemisphere, have been observed and caused by the global warming (Myneni et al., 1997; Schaber and Badeck, 2005; Zhou et al., 2001). Moreover, the changes of vegetation phenology also affect carbon, water and energy exchanges between the vegetation and the atmosphere (White et al., 2009; Delbart et al., 2015; Both et al., 2009; Picard et al., 2005; Richardson et al., 2013). Such as earlier spring phenology would advance soil water depletion and enhance mid-summer drought in some cases (White and Nemani, 2003). Therefore, accurate observation of SOS is important to understand regional-to-global carbon budget and climate change (Piao et al., 2015; Zhang et al., 2017; Peng et al., 2017a,b,c). Although the use of ground observations by volunteers, scientists, and ground-based cameras is growing (Richardson et al., 2007; Sonnentag et al., 2012; Denny et al., 2014), satellite-based remote sensing is still widely used to monitor spring phenology because of its significant advantages with respect to

* Corresponding authors.
E-mail addresses: hefery@163.com (C. Wu), leyu@tsinghua.edu.cn (L. Yu).

https://doi.org/10.1016/j.agrformet.2018.03.010
Received 21 April 2017; Received in revised form 12 March 2018; Accepted 13 March 2018
Available online 20 March 2018
0168-1923/ © 2018 Elsevier B.V. All rights reserved.

synoptic coverage and repeated temporal sampling at regional and global scales (Myneni et al., 1997; Zhang et al., 2003; White et al., 2009; Gonsamo et al., 2012; Delbart et al., 2015). Various coarse-resolution remote sensing images are available to detect spring phenology from regional to global scales. Such as the advanced very high resolution radiometer (AVHRR) captures images and has the Normalized Difference Vegetation Index (NDVI) products at spatial resolutions between 1.1–8 km. These data are the coarsest and most commonly used satellite data for measuring spring phenology (White et al., 2009; Zhang et al., 2007, 2014; de Jong et al., 2011; Julien and Sobrino, 2009; Zhou et al., 2001), because they boast the longest and densest time series available with global coverage (time series begin ~1982). Other data used for phenology detection extend back about 10–17 years, which include the medium-resolution imaging spectrometer (MERIS) data (300 m), the moderate-resolution imaging spectroradiometer (MODIS) data (250 m–0.05°), and the Systeme Probatoire d'Observation de la Terre (SPOT) vegetation data (1 km) (Zhang et al., 2003; Fisher et al., 2006; White et al., 2009; Ganguly et al., 2010; Dash et al., 2010; Guyon et al., 2011). Landsat images with spatial resolutions of 30 m have temporal resolution of ~16 days, making them an impractical source for consistent annual time series of regional-scale phenology for most parts of the planet (Zhang et al., 2017).

Validation of the satellite-derived phenology products is an important and challenging task in remote sensing, but a primary challenge is to determine an appropriate method to scale up plot-level or finer resolution observations to the coarser resolution observations from many satellites (Buermann et al., 2002; de Beurs et al., 2009; Herold et al., 2008; Weiss et al., 2007). Previous studies have generally validated coarser resolution spring phenology data by averaging finer resolution data (Delbart et al., 2015; Román et al., 2011). Recently, a percentile approach was developed, and it was found that the 30th percentile of fine-resolution (30 m) phenology data corresponded best (i.e., had the smallest errors) to coarser resolution (500 m) spring phenology data (Zhang et al., 2017). This method reflects that spring greenup is not able to be captured by coarse-resolution data until the greenup has occurred in 30% of fine-resolution pixels, which also indicates that coarse-resolution greenup dates represents mostly the relatively early greenup values at fine-resolution pixels (Zhang et al., 2017). However, to our knowledge no studies have compared the results between averaged and percentile approaches. Zhang et al. (2017) pointed out that this type of comparison is needed to verify if the 30th percentile is always the optimal percentile across various landscapes and ecosystems. In addition, studies have rarely evaluated the methods of aggregating satellite-derived spring phenology data from finer to coarser spatial resolutions (from 250 m to 8 km), especially for large regions.

In this study, we used an ecoregions map over the contiguous United States to identity ecosystems at the province and division scale. We explored the relationships between finer (250 m) and coarser (8 km) resolution images and compared the average and percentile approaches for aggregating and scaling up the start of spring phenology (SOS).

2. Methods

2.1. Data

For our base phenology data, we used MOD13Q1 vegetation index data, which are provided every 16 days at a 250 m spatial resolution as a gridded level-3 product in sinusoidal projection. We did not use finer spatial resolution images (such as 30 m Landsat images) because of the long repeat cycle of observations (~16 days for Landsat). This coarse temporal resolution makes it impractical to consistently produce annual time series for phenology detections at a regional scale for full coverage across the continental United States (Zhang et al., 2017). It is because the time gap between two valid observations could be more than one month if an observation is of low quality on a particular day because of cloud cover or other impacts. Our MOD13Q1 data, in contrast, consisted of the best quality observations (e.g., low clouds, low view angle, high NDVI/EVI value) of daily observations, composited across 16-day increments. Thus, weather conditions had limited impacts on data. We acquired enhanced vegetation index (EVI) and the quality assessment (QA) information in 2007 and 2008 from ftp://ladsweb.nascom.nasa.gov/allData/6/. The MOD13Q1 Collection 6 algorithm uses pre-composited (8-day) surface reflectance data, as opposed to daily data, and uses a new robust 2–band EVI instead of a backup algorithm from soil adjusted vegetation index (SAVI) (Huete et al., 2002; Jiang et al., 2008; Didan, 2015). A cloud-free, nadir-view pixel with no residual atmospheric contamination produces the best quality pixels. Only the higher quality cloud-free data are retained for further compositing. The current surface reflectance employs a minimum blue band approach to minimize effects of aerosols and other contaminants (Huete et al., 2002; Jiang et al., 2008; Didan, 2015).

To quantify land cover type, we used the MODIS product MCD12Q1, which has a 500 m resolution and was produced using a supervised classification algorithm based on high-quality land cover training sites; training sites were developed using high-resolution imagery and ancillary data (Muchoney et al., 1999). We used the most recent version of MCD12Q1. The primary land cover scheme was provided by an International Geosphere-Biosphere Program (IGBP) land cover classification scheme (Friedl et al., 2010), which was used to calculate the indicators of landscape fragment (ILF).

For validation of our MOD13Q1-derived estimates of SOS phenology, we used MCD12Q2, which has a 500 m resolution, and is a MODIS Collection 5 product acquired from the combined TERRA and AQUA platforms. We downloaded these data from http://e4ftl01.cr.usgs.gov. MCD12Q2 primarily used MODIS EVI, which was computed from MODIS the nadir bidirectional reflectance distribution function (BRDF)-adjusted reflectance (NBAR). EVI was produced every 8 days using overlapping 16 day compositing windows, and there was a maximum of 46 possible EVI values for any year. Those time series underwent a gap-filling and smoothing process (Zhang et al., 2006; Ganguly et al., 2010). Phenophase transition dates were estimated by identifying local maxima and minima in the rate of change of curvature of the fitted logistic function (Zhang et al., 2003).

For ground-based observations, we used observations of first leaf of common lilac collected by the USA National Phenology Network (USA-NPN). The USA-NPN is a consortium of individuals and organizations that collect, share, and use phenology data, and aims to develop and distribute derived phenological information (Denny et al., 2014). USA-NPN lilac phenology data have been widely used in previous studies (Allstadt et al., 2015; Ault et al., 2015; Piao et al., 2015; Verger et al., 2016), and have been proven useful for providing species-specific phenological data (White et al., 2009; Kellermann et al., 2015; Glynn and Owen, 2015; Piao et al., 2015). We used lilac first leaf observations collected at 95 sites (Fig. 1) in 2007 (USA-NPN, 2015).

We quantified ecoregions of the continental United States (Fig. 1) based on data from the Forest and Rangeland Ecosystem Science Center. This data set categorized ecoregions at four levels, of which we used the three largest: (1) domains, the largest ecosystems; (2) divisions, which are differentiated based on precipitation and temperature; and (3) provinces, which are based on vegetation or other natural land covers (Bailey, 2004; Omernik and Bailey, 1997). In addition, vegetation in the same ecoregion has the similar climate and human conditions (Yang et al., 2017). In this study, we merged several closely related divisions to get six divisions as shown in Fig.1.

2.2. SOS estimation from MODIS EVI

For MOD13Q1 data, pixels contaminated by cloud, aerosols, and other contaminants were marked as invalid and removed; the remaining EVI data in 2007 and 2008 across the continental United States were aggregated across 250 m resolution pixels within 35 × 35-pixel

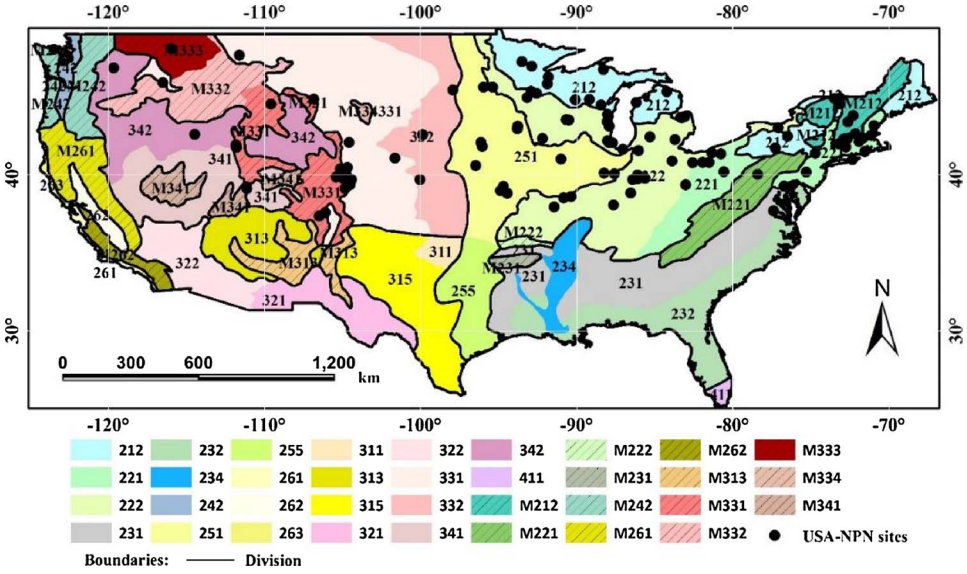

Fig. 1. Spatial distribution of in situ observations (USA-NPN sites) superimposed over an ecoregions map. Six divisions include warm or hot continental division (W/HD), subtropical or savanna (411) division (S/SD), prairie division (PD), tropical/subtropical steppe or tropical/subtropical desert division (TSS/TSDD), temperate steppe or temperate desert (TSD/TDD), and marine regime mountains or Mediterranean division (M/MD). The province level ecoregion include Laurentian mixed forest province (212), eastern broadleaf forest (oceanic) province (221), eastern broadleaf forest (continental) province (222), southeastern mixed forest province (231), outer coastal plain mixed forest province (232), lower Mississippi riverine forest province (234), pacific lowland mixed forest province (242), prairie parkland (temperate) province (251), prairie parkland (subtropical) province (255), California coastal chaparral forest and shrub province (261), California dry steppe province (262), California coastal steppe-mixed forest-redwood forest province (263), great plains steppe and shrub province (311), Colorado plateau semi-desert province(313), southwest plateau and plains dry steppe and shrub province (315), Chihuahuan semi-desert province (321), American semi-desert and desert province (322), great plains-Palouse dry steppe province (331), great plains steppe province (332), intermountain semi-desert and desert province (341), intermountain semi-desert province (342), everglades province (411), Adirondack-New England mixed forest-coniferous forest-alpine meadow province (M212), central Appalachian broadleaf forest-coniferous forest-meadow province (M221), Ozark broadleaf forest - meadow province (M222), Ouachita mixed forest - meadow province (M231), Cascade mixed forest-coniferous forest-alpine meadow province (M242), Sierran steppe-mixed forest-coniferous forest-alpine meadow province (M261), California coastal range open woodland-shrub-coniferous forest-meadow province (M262), Arizona-New Mexico mountains semi-desert-open woodland-coniferous forest-alpine meadow province (M313), southern rocky mountain steppe-open woodland-coniferous forest-alpine meadow province (M331), middle rocky mountain steppe-coniferous forest-alpine meadow province (M332), northern rocky mountain forest-steppe-coniferous forest-alpine meadow province (M333), Black Hills coniferous forest province (M334), and Nevada-Utah mountains-semi-desert-coniferous forest-alpine meadow province (M341).

windows. This window size (~8 km) corresponds to the spatial resolution of AVHRR images, such as GIMMS NDVI3. We used piecewise logistic models to calculate SOS phenology over continental United States for 2007 and 2008 at both resolutions: fine-scale "SOS (250 m)" and aggregated coarse-scale "SOS (8 km)."

Piecewise logistic models provided bounded and continuous functions for modeling growth processes; and each parameter could correspond with a biophysical meaning related to vegetation growth (Zhang, 2015). Many previous studies have shown that logistical models tend to perform superior to both Fourier-based and asymmetric Gaussian functions for fitting remote sensing-derived phenology data (Beck et al., 2006; Zhang, 2015). Piecewise logistic models can effectively depict the seasonality of satellite-observed greenness across various ecosystems (Zhang et al., 2003, 2006). This method has been applied to investigate seasonal vegetation growth using ground-based webcam data (Richardson et al., 2006; Kovalskyy et al., 2012), Landsat data (Fisher et al., 2006; Kovalskyy et al., 2012), AVHRR data (Zhang et al., 2007; Julien and Sobrino, 2009), and MODIS data (Zhang et al., 2003, 2006; Liang et al., 2011).

2.3. Comparison of the percentile and average approaches for spring phenology aggregation

We statistically compared SOS (250 m) with SOS (8 km) using average absolute difference (AAD, Eq. (1)), mean difference (BIAS, Eq. (2)), root mean square error (or difference) (RMSE or RMSD, Eq. (3)), and linear regression. AAD measured statistical dispersion equal to the average absolute difference of SOS (250 m) and SOS (8 km). BIAS evaluated the overestimation (positive BIAS) or underestimation (negative BIAS) of SOS (250 m) and SOS (8 km). RMSE was used to validate the estimated SOS in this study by comparing them to other satellite (MCD12Q2) and ground-based (USA-NPN) observations. RMSD evaluated the average uncertainty between SOS (250 m) and SOS (8 km), because SOS (250 m) and SOS (8 km) were remote sensing estimates without clear a priori references. Linear regression described the overall relationship between SOS (250 m) and SOS (8 km).

$$AAD = \frac{\sum_{i=1}^{N} |SOS_{250m} - SOS_{8km}|}{N} \quad (1)$$

$$BIAS = \frac{\sum_{i=1}^{N} (SOS_{250m} - SOS_{8km})}{N} \quad (2)$$

$$RMSE\,(/RMSD) = \sqrt{\frac{\sum_{i=1}^{N} (SOS_{250m} - SOS_{8km})^2}{N}} \quad (3)$$

where SOS_{8km} indicates the SOS value after aggregating across 35 × 35 pixels (i.e. ~8 km resolution), and SOS_{250m} indicates the SOS value with the original 250 m pixels.

We used two methods to aggregate SOS (250 m) to SOS (8 km): (1) by selecting the timing at a specific percentile at intervals of 5% within 35 × 35-pixel grids (i.e. different percentile approach), and (2) by averaging SOS across a 35 × 35-pixel grids (i.e. averaged approach) for all 250 m pixels. From a biophysical perspective, SOS from this percentile approach represents the date at which vegetation greenup has occurred in a certain percent of the original 250 m pixels, namely minimum SOS (close to 0.01%), 5%, 10%, 15%, … 100% (i.e. maximum SOS).

We extracted the minimum AAD and BIAS (i.e. most approached zero) based on the percentile approach (termed AAD_{Pmin} and $BIAS_{Pmin}$), and got the corresponding percentiles. Then, we compared the AAD_{Pmin} and $BIAS_{Pmin}$ to AAD and BIAS from the average approach (termed AAD_{Ave} and $BIAS_{Ave}$), respectively, to evaluate the two methods of aggregating SOS at the ~8 km scale, province scale, division scale, and national scale (see Fig. 1 for province and division scales, which were based on ecoregions). We identified the smaller AAD values from AAD_{Pmin} and AAD_{Ave} (termed $AAD_{(P+Ave)min}$), and the smaller values from $BIAS_{Pmin}$ and $BIAS_{Ave}$ (termed $BIAS_{(P+Ave)min}$), and also calculated the difference between AAD_{Ave} and AAD_{Pmin} (i.e. AAD_{Ave} - AAD_{Pmin}).

In addition, we used the indicators of landscape fragment (ILF) to examine the potential factors that could explain the spatial distributions of AAD between SOS (250 m) and SOS (8 km) at different levels of spatial heterogeneity in land cover type. The five levels of

heterogeneities in ~8 km grids were determined using the proportion of SOS (250 m) ILF frequency (PILF) at intervals of 20%; 0–20% PILF represents the most homogeneous level, whereas 80–100% PILF indicates the most heterogeneous level.

We resampled MODIS land cover type data to the resolution of the MOD13Q1 data (250 m), and then calculated the ILF (Eq. (4)) (Zhan et al., 2004) in 35 × 35-pixel grids (~8 km resolution, with each pixel 250 m).

$$ILF = \frac{(N_f - 1)}{N_c} \quad (4)$$

$$N_c = \frac{A_t}{A_p} \quad (5)$$

where N_f is the total number of patches for all land cover types, and N_c is the ratio of the area in a 35 × 35-pixel grid (A_t) to the area of minimum patch (A_p) in a 35 × 35-pixel grid, where each pixel is 250 m.

3. Results and discussion

3.1. SOS validation

Fig. 2 shows the geographical distributions of SOS phenology (day-of-year, DOY) in 2007 estimated using MODIS EVI data (specifically, MOD13Q1) at 250 m resolution. It was found that earlier SOS (~70 day-of-year, DOY) in southern locations, and later SOS (~100 DOY) in northeastern continental United States. The latest SOS (> 130 DOY) was observed in north-central regions and mountain areas. Because spring temperature has been proven as the major driver for SOS values, vegetation at high latitudes or high altitudes generally requires a longer time for the accumulation of a certain amount of heat to trigger spring leaf onset (Menzel et al., 2006; Harrington et al., 2010; Barichivich et al., 2013; Piao et al., 2015). Thus the later SOS was observed in northern continental United States and mountain area. SOS values were missing across much of the western and southwestern continental United States; these areas are covered by evergreen forest and barren or sparse vegetation that change little in greenness from season to season, making it is difficult to calculate plant phenological metrics from satellite data (Guyon et al., 2011; Hufkens et al., 2012; Melaas et al., 2013; Shen et al., 2014 ; Liu et al., 2016).

Our estimates of SOS phenology from MOD13Q1 were significantly correlated with SOS estimates derived from widely used MCD12Q2 phenology product ($R = 0.74$, $p < 0.001$) and with ground-based observations of lilac first leaf ($R = 0.61$, $p < 0.001$) (Fig. 3); the corresponding RMSE values were 17.9 days and 17.5 days. White et al. (2009) found that estimating SOS differed by more than one month among 10 phenology detection methods, and the current major SOS products have the RMSE values of ~20 days compared to ground observations (Peng et al., 2017a). Compared to previous products, our estimating SOS has a little smaller error.

3.2. Evaluation of spring phenology aggregation methods at different scales

3.2.1. Pixel (~8 km) scale

At the pixel scale (i.e. in ~8 km grid), both $AAD_{(P+Ave)min}$ and $BIAS_{(P+Ave)min}$ were less than 1 day across 80% of the continental United States, and less than 5 day across 95% of the continental United States (Fig. 4). Relatively large $AAD_{(P+Ave)min}$ and $BIAS_{(P+Ave)min}$ values occurred in the western and southern areas of the continental United States, and in the riverine forests of the lower Mississippi (province 234) (Fig. 4).

Because $AAD_{(P+Ave)min}$ and $BIAS_{(P+Ave)min}$ showed identical t spatial distributions and statistical results, we only presented the spatial distributions of $AAD_{(P+Ave)min}$ and the corresponding statistical results in Fig. 5. Compared with the percentile approach for aggregating SOS (250 m), the average approach yielded smaller AAD values over 23% of total land area of the continental United States, mostly the north-central and northeastern regions. The percentile approach yielded smaller AAD values over the remainder of the continental United States, particularly in western, southern, and central regions. Across 45% of the total land area, SOS was optimally aggregated using the timing of 20th–50th percentile of SOS (250 m) (Fig. 5).

AAD values from the average approach were larger than the minimum AAD values from the percentile approach for 65% of the continental United States (Fig. 6). The differences between AAD values derived from the two approaches were generally very small—e.g., less than 2 days for 60% of the continental United States and less than 5 days for 78% of the continental United States.

3.2.2. Ecoregion at the province scale

At the ecoregion province scale AAD varied more than fivefold (even tenfold) (Fig. 7), if SOS (250 m) was aggregated to SOS (8 km) using different percentiles or average approaches. AAD was very large if SOS was aggregated from either < 10th or > 90th percentile of SOS (250 m) within ~8 km grids. For example, in the Laurentian mixed forest province (212), AAD was 31 days or 34 days when SOS was obtained using 100th or 0.01th percentile of SOS (250 m). However, AAD reached the minimum AAD (i.e. AAD_{Pmin}) if SOS was aggregated from an optimal percentile, such as 45th percentile of SOS (250 m) for Laurentian mixed forest province (212) in warm or hot continental division (W/HD). This AAD was 1.94 days, which was close to the AAD (1.89 days) derived from the average approach (Fig. 7).

For the percentile approach, the lowest AAD (AAD_{Pmin}) generally

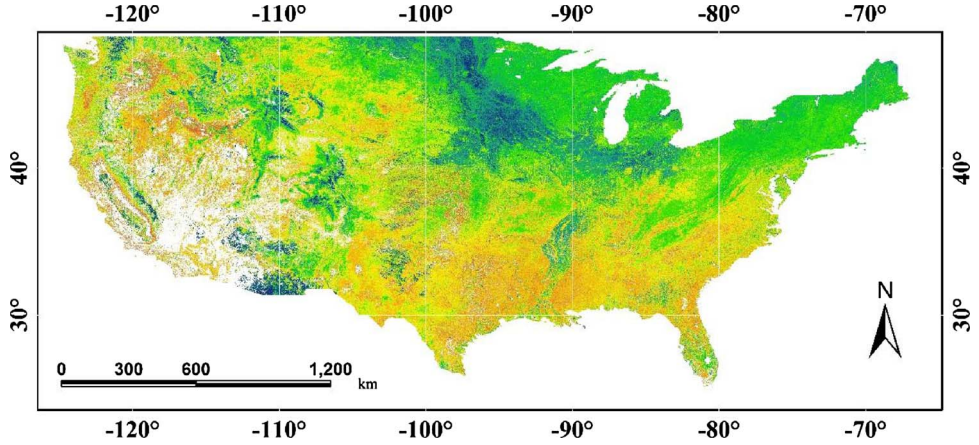

Fig. 2. Start of spring phenology (SOS, day-of-year, DOY) in 2007 across the contiguous United States, estimating by MODIS enhanced vegetation index (EVI) (specifically, MOD13Q1) with the spatial resolution of 250 m.

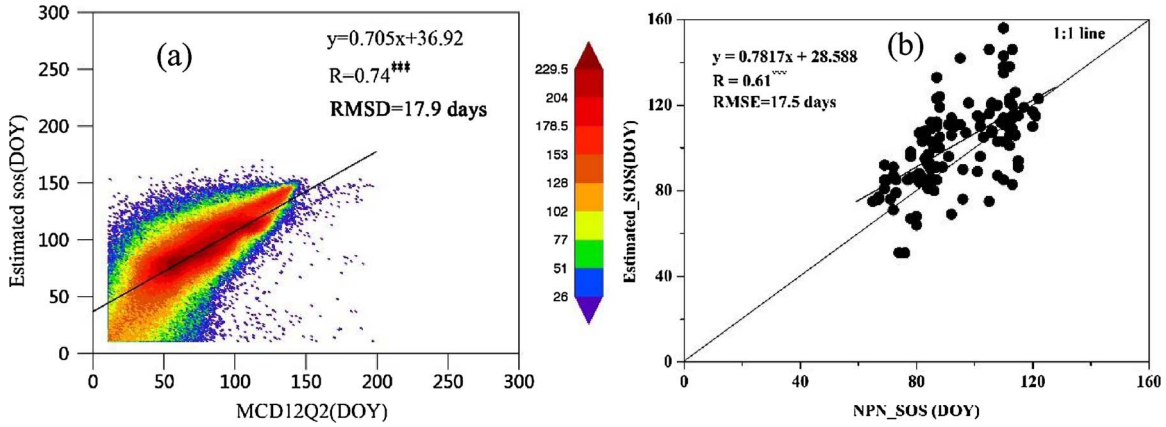

Fig. 3. Validation of MOD13Q1-derived estimates of start of spring phenology (SOS, day-of-year, DOY) (i.e. Estimated_SOS) in 2007 by comparing them to: (a) MCD12Q2-derived SOS, and (b) ground-based observations of lilac first leaf (i.e. NPN_SOS).

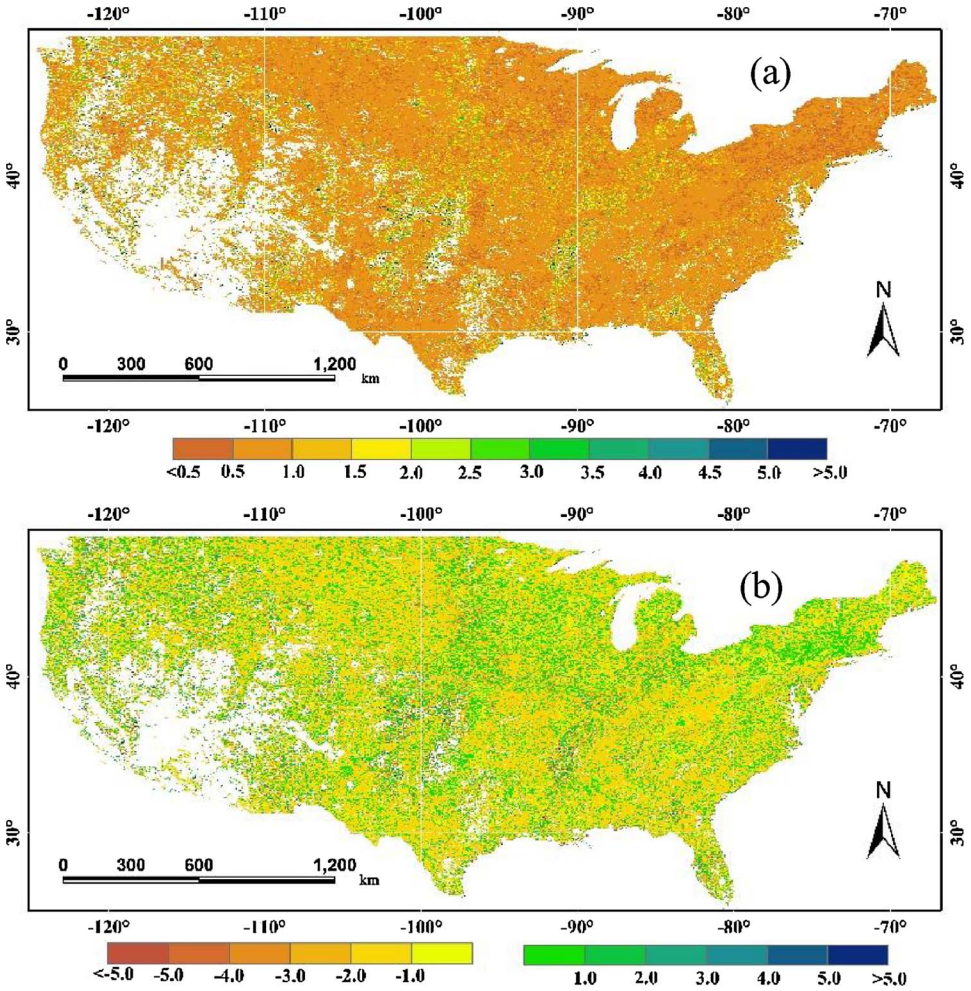

Fig. 4. The minimum average absolute difference (AAD) (a) and BIAS (b) in 2007 between SOS (250 m) and SOS (8 km) aggregated using percentile or average approaches, termed as $AAD_{(P+Ave)min}$ (a) and $BIAS_{(P+Ave)min}$ (b).

occurred around the 40th percentile at the ecoregion province scale, and AAD_{Pmin} values were mainly less than 5 days. However, there were several exceptions, such as Everglades province (411, AAD_{Pmin} = 17.33 days), for which AAD_{Pmin} occurred at the timing of 60th percentile of SOS (250 m). Other exceptions included the prairie parkland (subtropical) province (255) (percentile = 25th and AAD_{Pmin} = 10.86 days), California coastal steppe-mixed forest-redwood forest province (263) (percentile = 20th and AAD_{Pmin} = 11.88 days), intermountain semi-desert and desert province (341) (percentile = 55th and AAD_{Pmin} = 15.31 days), Nevada-Utah mountains-semi-desert-coniferous forest-alpine meadow province (M341) (percentile = 50th and AAD_{Pmin} = 15.29 days), great plains steppe and shrub province (311) (percentile = 15th and AAD_{Pmin} = 14.72 days), Colorado plateau semi-desert province (313) (percentile = 55th and AAD_{Pmin} = 18.33 days), and American semi-desert and desert province (322) (percentile = 70th and AAD_{Pmin} = 15.71 days) (Fig. 7).

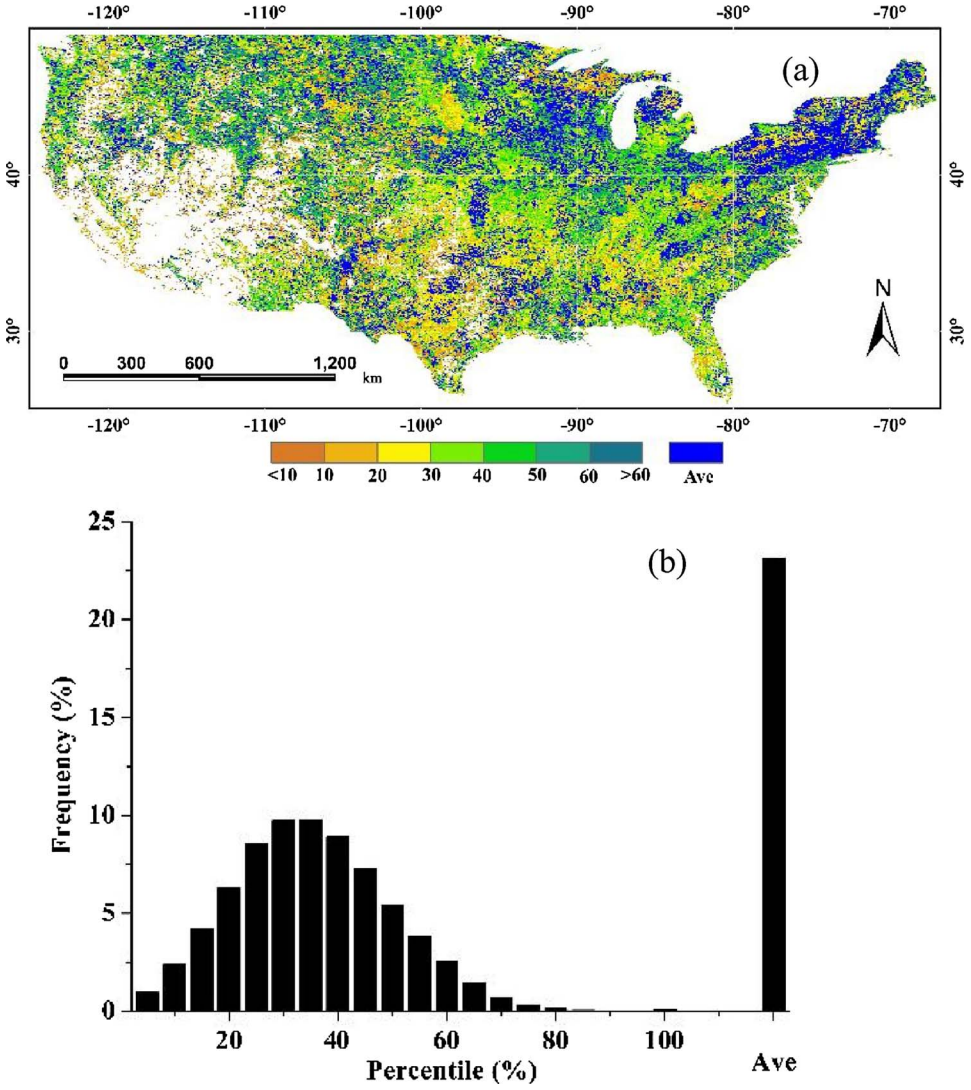

Fig. 5. The distribution of areas where the percentile and average (Ave) approaches yielded the minimum average absolute difference (AAD) (termed as $AAD_{(P+Ave)min}$) in 2007 over the contiguous United States (a), and the frequency distribution of the percentile and average approaches with the $AAD_{(P+Ave)min}$ (b). $AAD_{(P+Ave)min}$ identified the aggregation approach (average or percentile) that yielded the smallest difference between SOS (250 m) and SOS (8 km).

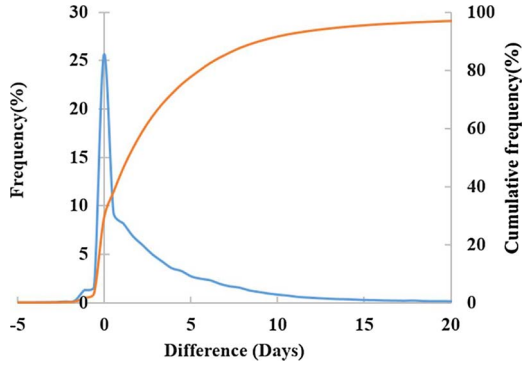

Fig. 6. The frequency distribution of the difference between average absolute difference (AAD) derived from the average approach (termed as AAD_{Ave}) and the minimum AAD from the percentile approach (termed as AAD_{Pmin}) in 2007, i.e AAD_{Ave} - AAD_{Pmin}. AAD was calculated as the difference between SOS (250 m) and SOS (8 km), and was calculated separately for values of SOS (8 km) resulting from different aggregation methods (i.e., percentile and average approaches).

The AAD from the average approach (AAD_{Ave}) was generally close to AAD_{Pmin} using different percentiles; the differences were generally less than 0.5 day, except for above-mentioned exceptions. In addition, there were seven provinces where AAD values from average approach were less than the AAD_{Pmin} from percentile approach; these provinces included Laurentian mixed forest province (212), eastern broadleaf forest (oceanic) province (221), Adirondack-New England mixed forest-coniferous forest-alpine meadow province (M212), central Appalachian broadleaf forest-coniferous forest-meadow province (M221), great plains-Palouse dry steppe province (331), middle rocky mountain steppe-coniferous forest-alpine meadow province (M332), and Black Hills coniferous forest province (M334) (Fig. 7).

Generally, negative BIAS occurred if SOS (8 km) was derived using the percentile approach with percentiles less than the 35th percentile, while positive BIAS mainly occurred if SOS (8 km) was derived using the 40th to 100th percentiles (Fig. 8). This pattern held for most provinces, with the exception of the same provinces mentioned earlier as exceptions for AAD_{Pmin}. These provinces included 255, 263, M261, 341, M341, 311, 313, 322, and 411. Negative BIAS values reached as high as 40 days and positive BIAS values reached as high as 70 days. Overall, aggregation using roughly the 35th percentile achieved BIAS values that approached zero (Fig. 8). Compared to the percentile approach, BIAS values resulting from the average approach to aggregation were close to the minimum BIAS (i.e. $BIAS_{Pmin}$ approached zero), except for provinces 255, 263, M261, 341, M341, 311, 313, 322, and 411 (Fig. 8).

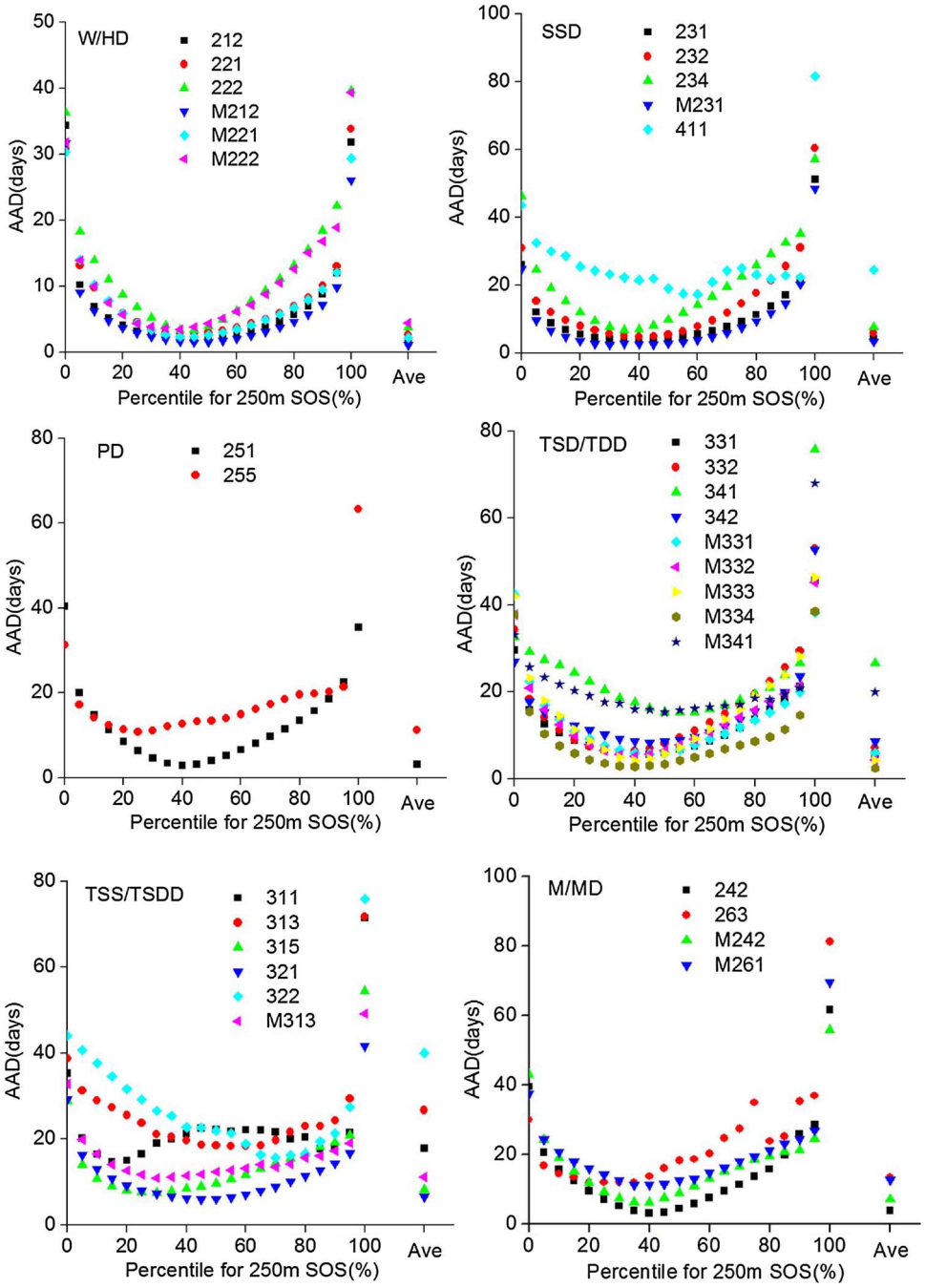

Fig. 7. At the province scale, average absolute difference (AAD) in 2007 between SOS (250 m) and SOS (8 km) derived by different aggregation methods—e.g., percentile and average (Ave) approaches.

3.2.3. Ecoregion at the division scale

At the ecoregion division scale, AAD and BIAS between SOS (250 m) and SOS (8 km) were relatively consistent among six divisions. The minimum AAD (i.e. AAD_{Pmin}) values were around 2.78 days in warm or hot continental division (W/HD), 4.93 days in subtropical or savanna division (S/SD), 5.40 days in prairie division (PD), 7.01 days in temperate steppe or temperate desert (TSD/TDD), while 10.80 days in tropical/subtropical steppe or tropical/subtropical desert division (TSS/TSDD) and 13.36 days in marine regime mountains or Mediterranean division (M/MD). The AAD_{Pmin} was found for aggregation using 40th percentile of SOS (250 m) (Fig. 9a), and the BIAS generally approached zero for aggregation using the 35th percentile of SOS (250 m) (Fig. 9b), although BIAS approached zero in TSS/TSDD and M/MD divisions for aggregation using the 15th percentile (Fig. 9b).

The AAD from average approach (AAD_{Ave}) was less than the AAD_{Pmin} based on the percentile approach in division PD but it was larger in other divisions. Specifically, the difference between AAD_{Pmin} and AAD_{Ave} was smallest in W/HD (0.04 days), and then followed by PD (0.19 days), S/SD (0.59 days), TSD/TDD (0.91 days), TSS/TSDD (2.06 days), and M/MD (2.11 days) (Fig. 9).

3.2.4. National scale

At the national scale the minimum AAD (AAD_{Ave}) values (6.39 days) occurred when aggregation using the 40th percentile of SOS (250 m) (Fig. 10), and the BIAS approached zero when aggregation using the 30th percentile of SOS (250 m) (Fig. 10). The difference between AAD_{Ave} (7.43 days) and AAD_{Pmin} (6.39 days) was 1.04 days.

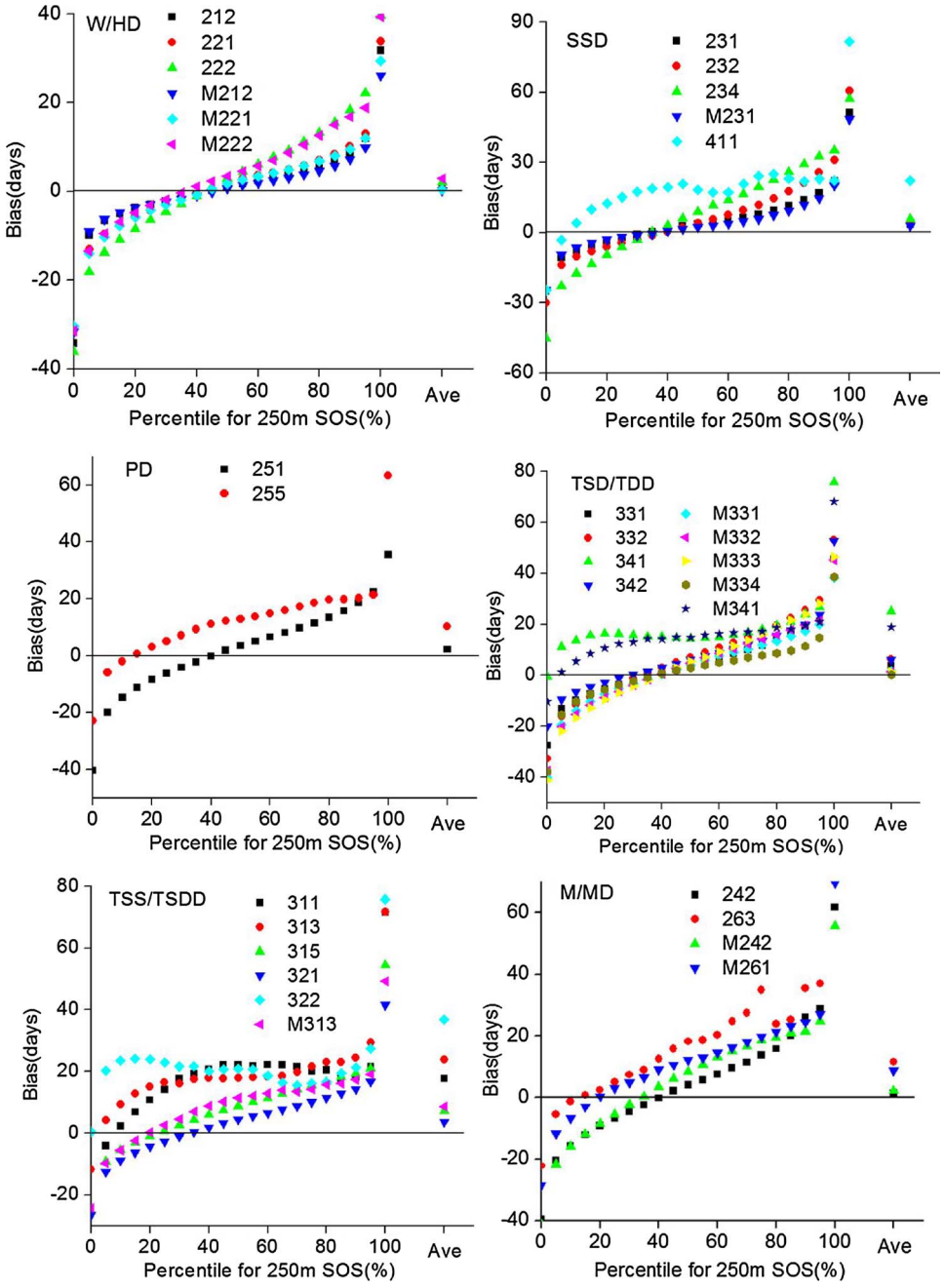

Fig. 8. At the province scale, BIAS in 2007 between SOS (250 m) and SOS (8 km) derived by different aggregation methods—e.g., percentile and average (Ave) approaches.

3.3. Comparisons of SOS at the different heterogeneity scales

In homogeneous regions (low PILF values), SOS (250 m) and SOS (8 km) values were closely related, distributed along the 1:1 line with the slopes close to 1 day (Fig. 11). With increases in heterogeneity (higher PILF values), the intercepts in the linear regressions increased, the slopes decreased, and the correlation coefficients declined from 0.78 to 0.65. AAD was 8.37 days and RMSD was 16.76 days in homogeneous regions (PILF < 20%). In the most heterogeneous regions (PILF = 80–100%), AAD was 9.97 days and RMSD was 18.43 days. If all the good SOS pixels across the regions were considered (PILF = 0–100%), then the AAD and RMSD values were 9.23 days and 17.74 days, respectively, and the correlation coefficient was 0.71.

AAD (or BIAS) values in eastern parts of the continental United States were smaller than values in western and southern regions of the continental United States. Zhang et al. (2017) found that the heterogeneity played a notable role affecting AAD values, which measure the difference between SOS derived from finer and coarser resolution images. Our results also indicated that AAD values tended to be larger in heterogeneous regions and smaller in homogeneous regions (Fig. 11). In addition, the poor accuracy and missing values of SOS likely contributed to relatively large AAD values in western and southern regions of the continental United States, so that large AAD and BIAS values appeared in the areas with many low accuracy or invalid SOS (250 m) pixels. Besides the SOS estimated in this study, many current land surface phenology products also fail to estimate SOS in western and southern regions of the continental United States—these products include MCD12Q2 (Zhang et al., 2006; Ganguly et al., 2010), Global Vegetation Index and Phenology Multi-sensor Phenology (White et al., 2009; Didan, 2010; Didan et al., 2016), Global Long-Term Climate Modeling Grid Land Surface Phenology (Zhang et al., 2014; Zhang, 2015), and other products (Morisette et al., 2009; Tan et al.,

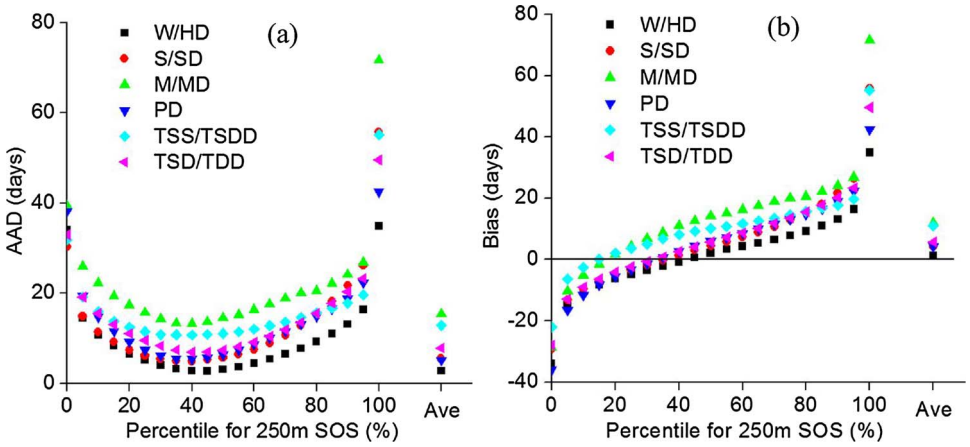

Fig. 9. At the division scale, average absolute difference (AAD) (a) and BIAS (b) in 2007 between SOS (250 m) and SOS (8 km) derived by different aggregation methods—i.e., percentile and average (Ave) approaches in six ecoregion divisions.

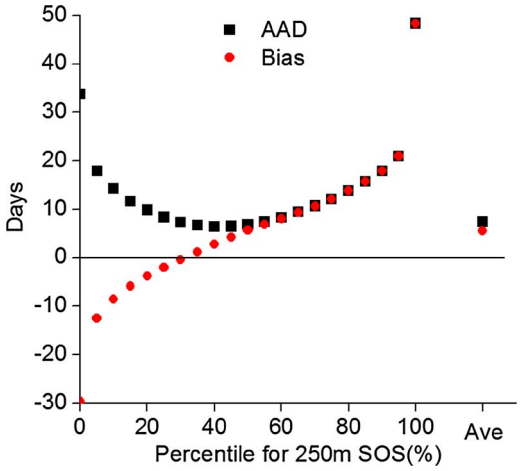

Fig. 10. At the national scale, average absolute difference (AAD) (a) and BIAS (b) in 2007 between SOS (250 m) and SOS (8 km) derived by different aggregation methods—i.e., percentile and average (Ave) approaches.

2008; Tan et al., 2011; Reed et al., 1994). This failure can be attributed to the ecosystem processes and vegetation types in these regions (White et al., 2009; Gonsamo et al., 2012; Hmimina et al., 2013; Melaas et al., 2015). Satellites have difficulty in detecting the subtle greenness changes in evergreen forests or barren or sparsely vegetated areas common in western and southern regions, whereas satellites provide best estimates of land surface phenology in seasonal, deciduous forests, where seasonal changes in greenness are dramatic (Baldocchi et al., 2005; Zhang et al., 2006; Kamel et al., 2008; Garrity et al., 2011; Guyon et al., 2011; Gonsamo et al., 2012; Hufkens et al., 2012; Hmimina et al., 2013; Melaas et al., 2013; Ryu et al., 2014; Wu and Chen, 2014; Shen et al., 2014; Liu et al., 2016).

3.4. Interannual variability in scaling spring phenology

We compared analyses scaling up spring phenology in 2008 and 2007 to investigate interannual variability in scaling up spring phenology. We found similar patterns of spatial distribution of AAD values—i.e. AAD values were low over most of the continental United States, and AAD values were relatively large in western and southern regions of the continental United States and in the lower Mississippi riverine forest province (234) (Fig. 12a). In 2008, the average approach for aggregation yielded the lowest AAD ($AAD_{(P+Ave)min}$) for 4% of the continental United States area, while the percentile approach yielded the lowest AAD values for the vast majority of locations. Across 60% of the continental United States area, the $AAD_{(P+Ave)min}$ was concentrated within the 30th–50th percentiles (Fig. 12b). AAD values using the average approach were generally larger than those achieved using percentile approach (for 77% of the continental United States area). However, the difference in AAD between the two approaches was less than 2 days for 55% of the continental United States, and was less than 5 days for 75% of the continental United States. (Fig. 12c), indicating that the two approaches tended to yield similar results. We found similar spatial distribution of $AAD_{(P+Ave)min}$ and the optimal percentiles (concentrated within 30th–45th) in 2007 and 2008. Although the area with $AAD_{(P+Ave)min}$ (average approach) arose from 4% in 2008 to 23% in 2007 (23%), the percentile approach generally performed better over more of the continental United States, and the difference between the two approaches was small in both years.

We also explored potential causes of this year-to-year variation. Based on the results in this study and a previous study (Zhang et al., 2017), landscape fragmentation appears to play an important role on spring phenology aggregation, and could contribute to interannual variation. Many other factors—especially climate factors such as temperature, precipitation, and cloud cover—could also contribute to changes in SOS from year to year (Westerling et al., 2006; Rosenzweig et al., 2007; Piao et al., 2015; Mazer et al., 2015; Wu et al., 2016). All of these factors could in turn cause large AAD values for SOS estimates when scaling finer resolution observations up to coarser resolution estimates of SOS. For example, in the southwestern continental United States, where barren or sparsely vegetated pixels are dominant, vegetation could grow well in wet years, while green vegetation may be undetectable from satellites in drought years. In the southern continental United States, cloud cover can contaminate satellite observations for periods longer than a month in some years, which hampers the ability of satellite data to reliably reconstruct vegetation growth and phenology. Human activities, such as the timing of agricultural planting and irrigation, could also change crop phenology (Xiao et al., 2013; Ding et al., 2016). Changes in any of these factors could cause changes in seasonal vegetation patterns between years, and in turn yield different SOS values.

3.5. The importance of scaling up spring phenology at multiple scales

Our evaluation of methods to scale up satellite-based spring phenology measurements (SOS) indicated that the optimal method for aggregating finer scale data—i.e., SOS (250 m)—varied across scales and regions of the continental United States. With respect to the AAD (or BIAS) between SOS (250 m) and SOS (8 km), strong patterns of spatial variation at the 8 km scale diminished when analyzed at larger ecoregion or national scales. This implies that scaling up spring

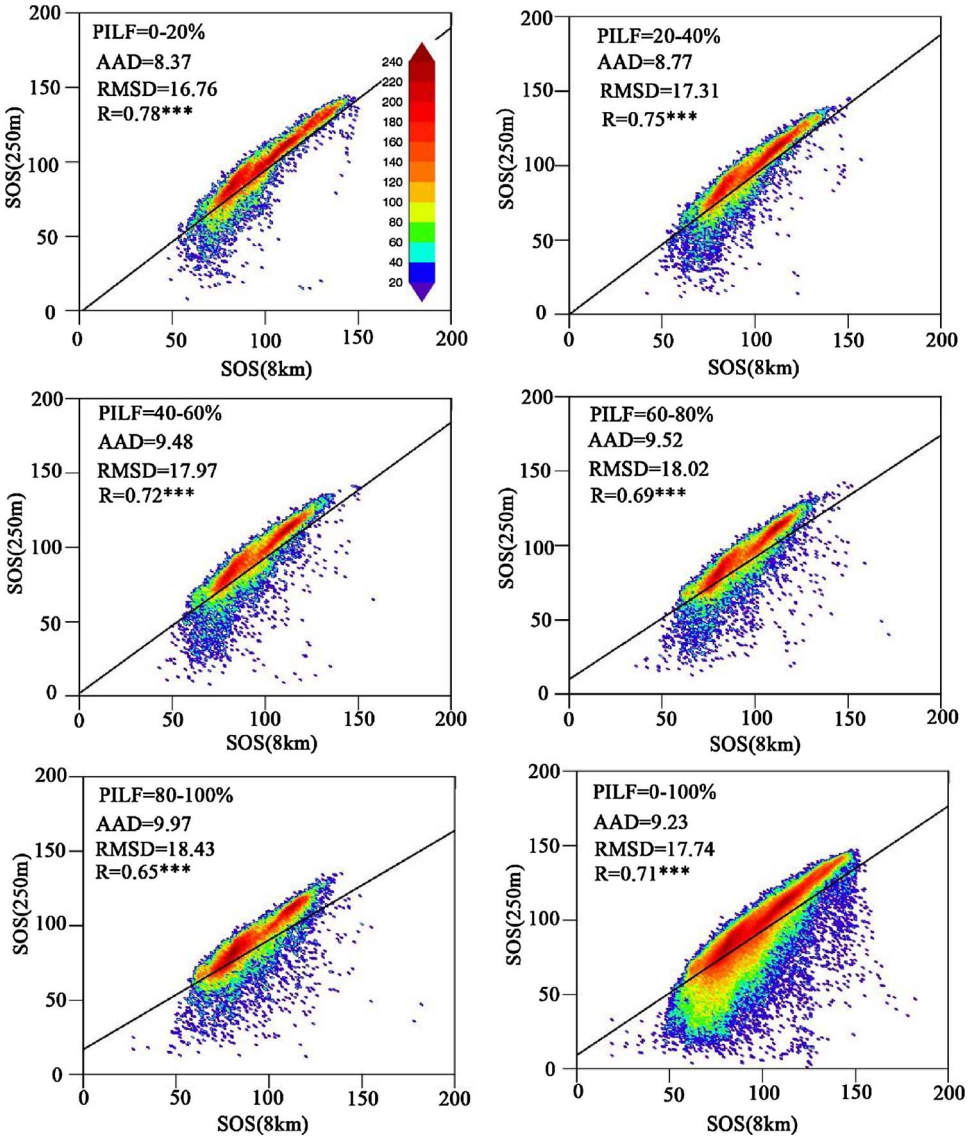

Fig. 11. Scatterplots of SOS (250 m) and SOS (8 km) in 2007 at different levels of landscape heterogeneity, represented by different proportions of indicators of landscape fragment (PILF) values. The tone level in the top left corner shows the density of scatter points. SOS (8 km) values were derived using the average (not percentile) approach. (For interpretation of the references to colour in this figure legend, the reader is referred to the web version of this article.)

phenology across large areas could smooth the spatial variance among SOS values detected at finer scales, which showed the importance of evaluating the scaling of phenology at multiple scales. Indeed, different results were yielded in the evaluations of scaling from 250 m to 8 km and to ecoregions or national scales.

The detailed distribution of AAD (or BIAS) can help identify the appropriate method to validate the SOS products derived from remote sensing images. For example, in places with large AAD (or BIAS), high-density ground observations may the best method for validating phenology products, to avoid factors that may be confounding remote sensing observations of phenology.

4. Conclusions

In this study, we calculated SOS (250 m) across the continental United States using Collection 6 MOD13Q1 EVI data. We then compared the average and percentile approaches for scaling up SOS (250 m) to SOS (8 km), and then to ecosystems and national scales. We used AAD and other error parameters to measure the difference between SOS (250 m) and SOS (8 km), to evaluate two approaches of scaling up spring phenology derived from remote sensing images. We also examined indicators of landscape fragment (ILF) that can explain the spatial distributions of AAD between SOS (250 m) and SOS (8 km). We found that the difference between the AAD from average and percentile approaches were very small; more detailed patterns of spatial variation at the 8-km scale were greatly reduced at larger ecoregion or national scales; the landscape heterogeneity played a notable role in AAD values between finer and coarser resolution images; and the scaling up SOS phenology were relatively consistent from year to year. In contrast to the relatively simple calculation in average approach, the percentile approach requires more complex calculations and the optimal percentile varies in different landscapes and ecosystems (although the optimal percentile usually occurred within the 30–50 th percentiles). For researchers who want the highest quality data for specific areas, we suggest they calculate both the average and percentiles and select the method that minimizes the errors for the selected area. However, for most researchers, use of the simpler average approach will be adequate, especially at larger scales.

Acknowledgements

The authors acknowledge Jake Weltzin (USA National Phenology

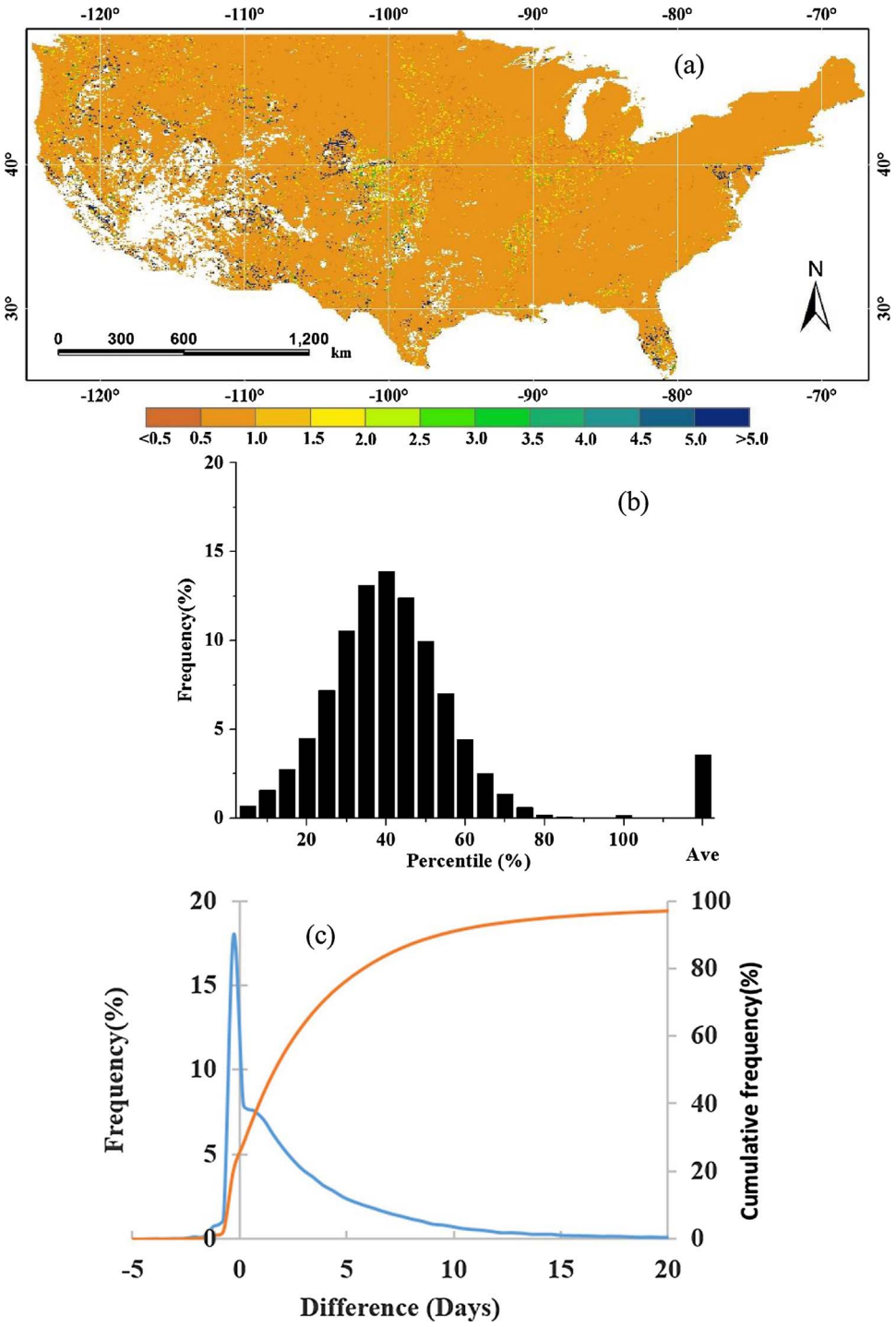

Fig. 12. The minimum average absolute difference (AAD) (termed as $AAD_{(P+Ave)min}$) in 2008 (a) between SOS (250 m) and SOS (8 km) derived by different aggregation methods—i.e., percentile and average approaches. (b) The frequency distribution of $AAD_{(P+Ave)min}$. (c) The frequency distribution of the difference between AAD from the average approach (termed as AAD_{Ave}) and the minimum AAD from the percentile approach (termed as AAD_{Pmin}).

Network) for the following data support: Lilac/honeysuckle data were provided by the USA National Phenology Network, Joseph M. Caprio, Mark D. Schwartz, and all contributors to past U.S. Dept. of Agriculture regional phenology projects; This study was supported by the National Key Research and Development Program of China [2016YFB0501501], National Natural Science Foundation of China [41325004, 41571423], Youth Innovation Promotion Association, Chinese Academy of Sciences [Y4YR1300QM], the key Research Program of Frontier Sciences, CAS to C. Wu [QYZDB-SSW-DQC011], and Director Foundation of Institute of Remote Sensing and Digital Earth, Chinese Academy of Sciences [Y6SJ020CX].

References

Allstadt, A.J., Vavrus, S.J., Heglund, P.J., Pidgeon, A.M., Thogmartin, W.E., Radeloff, V.C., 2015. Spring plant phenology and false springs in the conterminous US during the 21st century. Environ. Res. Lett. 10 (10), 104008.

Ault, T.R., Schwartz, M.D., Zurita-Milla, R., Weltzin, J.F., Betancourt, J.L., 2015. Trends and natural variability of spring onset in the coterminous United States as evaluated by a new gridded dataset of spring indices. J. Clim. 28 (21), 8363–8378.

Baldocchi, D.D., Black, T.A., Curtis, P.S., Falge, E., Fuentes, J.D., Granier, A., et al., 2005. Predicting the onset of net carbon uptake by deciduous forests with soil temperature

and climate data: a synthesis of FLUXNET data. Int. J. Biometeorol. 49 (6), 377–387.
Barichivich, J., Briffa, K.R., Myneni, R.B., Osborn, T.J., Melvin, T.M., Ciais, P., et al., 2013. Large-scale variations in the vegetation growing season and annual cycle of atmospheric CO2 at high northern latitudes from 1950 to 2011. Glob. Change Biol. 19, 3167–3183.
Bailey, R.G., 2004. Identifying ecoregion boundaries. Environ. Manage. 34, S14–S26.
Beck, P.S., Atzberger, C., Høgda, K.A., Johansen, B., Skidmore, A.K., 2006. Improved monitoring of vegetation dynamics at very high latitudes: a new method using MODIS NDVI. Remote Sens. Environ. 100 (3), 321–334.
Both, C., Van Asch, M., Bijlsma, R.G., Van Den Burg, A.B., Visser, M.E., 2009. Climate change and unequal phenological changes across four trophic levels: constraints or adaptations? J. Anim. Ecol. 78 (1), 73–83.
Buermann, W., Wang, Y.J., Dong, J.R., Zhou, L.M., Zeng, X.B., Dickinson, R.E., Potter, C.S., Myneni, R.B., 2002. Analysis of a multiyear global vegetation leaf area index data set. J. Geophys. Res.: Atmos. 107 (D22).
Dash, J., Jeganathan, C., Atkinson, P.M., 2010. The use of MERIS terrestrial chlorophyll index to study spatio−temporal variation in vegetation phenology over India. Remote Sens. Environ. 114 (7), 1388–1402.
de Jong, R., de Bruin, S., de Wit, A., Schaepman, M.E., Dent, D.L., 2011. Analysis of monotonic greening and browning trends from global NDVI time-series. Remote Sens. Environ. 115 (2), 692–702.
de Beurs, K.M., Wright, C.K., Henebry, G.M., 2009. Dual scale trend analysis for evaluating climatic and anthropogenic effects on the vegetated land surface in Russia and Kazakhstan. Environ. Res. Lett. 4 (4), 045012.
Delbart, N., Beaubien, E., Kergoat, L., Toan, T.L., 2015. Comparing land surface phenology with leafing and flowering observations from the PlantWatch citizen network. Remote Sens. Environ. 160, 273–280.
Denny, E.G., Gerst, K.L., Miller-Rushing, A.J., Tierney, G.L., Crimmins, T.M., Enquist, C.A., et al., 2014. Standardized phenology monitoring methods to track plant and animal activity for science and resource management applications. Int. J. Biometeorol. 58 (4), 591–601.
Didan, K., 2010. Multi−satellite earth science data record for studying global vegetation trends and changes. In: Honolulu, HI, USA. Proceedings of the 2010 International Geoscience and Remote Sensing Symposium 2530. pp. 2530.
Didan, K., Barreto, A.M., Miura, T., Tsend-Ayush, J., Zhang, X., Friedl, M., et al., 2016. Multi−Sensor Vegetation Index and Phenology Earth Science Data Records: Algorithm Theoretical Basis Document and User Guide Version 4.0. https://vip.arizona.edu/VIP_ATBD_UsersGuide.php, last accessed March 22nd, 2016. .
Didan, K., 2015. MOD13Q1 MODIS/Terra Vegetation Indices 16-Day L3 Global 250 m SIN Grid V006. NASA EOSDIS Land Processes DAAChttp://dx.doi.org/10.5067/MODIS/MOD13Q1.006.
Ding, D., Feng, H., Zhao, Y., He, J., Zou, Y., Jin, J., 2016. Modifying winter wheat sowing date as an adaptation to climate change on the loess plateau. Agron. J. 108, 53–63.
Fisher, J.I., Mustard, J.F., Vadeboncoeur, M.A., 2006. Green leaf phenology at Landsat resolution: scaling from the field to the satellite. Remote Sens. Environ. 100 (2), 265–279.
Friedl, M.A., Sulla-Menashe, D., Tan, B., Schneider, A., Ramankutty, N., Sibley, A., Huang, X., 2010. MODIScollection 5 global land cover: algorithm refinements and characterizationof new datasets. Remote Sens. Environ. 114 (1), 168–182.
Ganguly, S., Friedl, M.A., Tan, B., Zhang, X., &Verma, M., 2010. Land surface phenology from MODIS: characterization of the collection 5 global land cover dynamics product. Remote Sens. Environ. 114 (8), 1805–1816.
Garrity, S.R., Bohrer, G., Maurer, K.D., Mueller, K.L., Vogel, C.S., Curtis, P.S., 2011. A comparison of multiple phenology data sources for estimating seasonal transitions in deciduous forest carbon exchange. Agric. For. Meteorol. 151 (12), 1741–1752.
Glynn, P.D., Owen, T.W., 2015. Review of the USA National Phenology Network (No. 1411). US Geological Survey.
Guyon, D., Guillot, M., Vitasse, Y., Cardot, H., Hagolle, O., Delzon, S., Wigneron, J.P., 2011. Monitoring elevation variations in leaf phenology of deciduous broadleaf forests from SPOT/VEGETATION time-series. Remote Sens. Environ. 115 (2), 615–627.
Gonsamo, A., Chen, J.M., Wu, C., Dragoni, D., 2012. Predicting deciduous forest carbon uptake phenology by upscaling FLUXNET measurements using remote sensing data. Agric. For. Meteorol. 165, 127–135.
Harrington, C.A., Gould, P.J., St. Clair, J.B., 2010. Modeling the effects of winter environment on dormancy release of Douglas-fir. For. Ecol. Manage. 259, 798–808.
Herold, M., Woodcock, C.E., Loveland, T.R., Townshend, J., Brady, M., Steenmans, C., Schmullius, C.C., 2008. Land-cover observations as part of a global earth observation system of systems (GEOSS): progress, activities, and prospects. IEEE Syst. J. 2 (3), 414–423.
Hmimina, G., Dufrêne, E., Pontailler, J.Y., Delpierre, N., Aubinet, M., Caquet, B., et al., 2013. Evaluation of the potential of MODIS satellite data to predict vegetation phenology in different biomes: an investigation using groundbased NDVI measurements. Remote Sens. Environ. 132, 145–158.
Huete, A., Didan, K., Miura, T., Rodriguez, E.P., Gao, X., Ferreira, L.G., 2002. Overview of the radiometric and biophysical performance of the MODIS vegetation indices. Remote Sens. Environ. 83 (1), 195–213.
Hufkens, K., Friedl, M., Sonnentag, O., Braswell, B.H., Milliman, T., Richardson, A.D., 2012. Linking nearsurface and satellite remote sensingmeasurements of deciduous broadleaf forest phenology. Remote Sens. Environ. 117, 307–321.
Jiang, Z., Huete, A.R., Didan, K., Miura, T., 2008. Development of a twoband enhanced vegetation index without a blue band. Remote Sens. Environ. 112 (10), 3833–3845.
Julien, Y., Sobrino, J.A., 2009. Global land surface phenology trends from GIMMS database. Int. J. Remote Sens. 30 (13), 3495–3513.
Kamel, S., Guerric, le M., Eric, D., Christophe, F., Nicolas, D., Erwin, U., Sébastien, C., 2008. Evaluation of the onset of green−up in temperate deciduous broadleaf forests derived from moderate resolution imaging spectroradiometer (MODIS) data. Remote Sens. Environ. 112 (5), 2643–2655.
Kellermann, J.L., Enquist, C.A., Humple, D.L., Seavy, N.E., Rosemartin, A., Cormier, R.L., Barnett, L., 2015. A Bird's Eye view of the USA national phenology network. Phenological Synchrony and Bird Migration: Changing Climate and Seasonal Resources in North America 47. pp. 47.
Kovalskyy, V., Roy, D.P., Zhang, X.Y., Ju, J., 2012. The suitability of multi-temporal web-enabled Landsat data NDVI for phenological monitoring–a comparison with flux tower and MODIS NDVI. Remote Sens. Lett. 3 (4), 325–334.
Liang, L., Schwartz, M.D., Fei, S., 2011. Validating satellite phenology through intensive ground observation and landscape scaling in a mixed seasonal forest. Remote Sens. Environ. 115 (1), 143–157.
Linderholm, H.W., 2006. Growing season changes in the last century. Agric. For. Meteorol. 137 (1), 1–14.
Liu, Y., Wu, C., Peng, D., Xu, S., Gonsamo, A., Jassal, R.S., et al., 2016. Improved modeling of land surface phenology using MODIS land surface reflectance and temperature at evergreen needleleaf forests of central North America. Remote Sens. Environ. 176, 152–162.
Mazer, S.J., Gerst, K.L., Matthews, E.R., Evenden, A., 2015. Species-specific phenological responses to winter temperature and precipitation in a water-limited ecosystem. Ecosphere 6 (6), 1–27.
Melaas, E.K., Richardson, A.D., Friedl, M.A., Dragoni, D., Gough, C.M., Herbst, M., et al., 2013. Using FLUXNET data to improve models of springtime vegetation activity onset in forest ecosystems. Agric. For. Meteorol. 171, 46–56.
Melaas, E.K., Friedl, M.A., Richardson, A.D., 2015. Multiscale modeling of spring phenology across deciduous forests in the Eastern United States. Glob. Change Biol. 22 (6), 792–805.
Menzel, A., Sparks, T.H., Estrella, N., Koch, E., Aasa, A., Ahas, R., et al., 2006. European phenological response to climate change matches the warming pattern. Glob. Change Biol. 12 (10), 1969–1976.
Morisette, J.T., Richardson, A.D., Knapp, A.K., Fisher, J.I., Graham, E.A., Abatzoglou, J., et al., 2009. Tracking the rhythm of the seasons in the face of global change: phenological research in the 21st century. Front. Ecol. Environ. 7 (5), 253–260.
Myneni, R.B., Keeling, C.D., Tucker, C.J., Asrar, G., Nemani, R.R., 1997. Increased plant growth in the northern high latitudes from 1981 to 1991. Nature 386 (6626), 698–702.
Muchoney, D., Strahler, A., Hodges, J., LoCastro, J., 1999. The IGBP DISCover confidence sites and the system for terrestrial ecosystem parameterization: Tools for validating global land-cover data. Photogramm. Eng. Remote Sens. 65 (9), 1061–1067.
Omernik, J.M., Bailey, R.G., 1997. Distinguishing between watersheds and ecoregions. J. Am. Water Resour. Assoc. 33 (5), 935–949.
Peng, D., Zhang, X., Wu, C., Huang, W., Gonsamo, A., Huete, A.R., Didan, K., Tan, B., Liu, X., Zhang, B., 2017a. Intercomparison and evaluation of spring phenology products using National Phenology Network and AmeriFlux observations in the contiguous United States. Agric. Forest Meteorol. 242, 33–46.
Peng, D., Zhang, X., Zhang, B., Liu, L., Liu, X., Huete, A.R., et al., 2017b. Scaling effects on spring phenology detections from MODIS data at multiple spatial resolutions over the contiguous United States. ISPRS J. Photogramm. Remote Sens. 132, 185–198.
Peng, D., Wu, C., Li, C., Zhang, X., Liu, Z., Ye, H., et al., 2017c. Spring green-up phenology products derived from MODIS NDVI and EVI: intercomparison, interpretation and validation using National Phenology Network and AmeriFlux observations. Ecol. Indic. 77, 323–336.
Picard, G., Quegan, S., Delbart, N., Lomas, M.R., Toan, T., Woodward, F., 2005. Bud-burst modelling in Siberia and its impact on quantifying the carbon budget. Glob. Change Biol. 11 (12), 2164–2176.
Piao, S., Tan, J., Chen, A., Fu, Y.H., Ciais, P., Liu, Q., et al., 2015. Leaf onset in the Northern Hemisphere triggered by daytime temperature. Nat. Commun. 6.
Reed, B.C., Brown, J.F., VanderZee, D., Loveland, T.R., Merchant, J.W., Ohlen, D.O., 1994. Measuring phenological variability from satellite imagery. J. Veg. Sci. 5 (5), 703–714.
Richardson, A.D., Bailey, A.S., Denny, E.G., Martin, C.W., O'KEEFE, J.O.H.N., 2006. Phenology of a northern hardwood forest canopy. Glob. Change Biol. 12 (7), 1174–1188.
Richardson, A.D., Jenkins, J.P., Braswell, B.H., Hollinger, D.Y., Ollinger, S.V., Smith, M.L., 2007. Use of digital webcam images to track spring green-up in a deciduous broadleaf forest. Oecologia 152 (2), 323–334.
Richardson, A.D., Keenan, T.F., Migliavacca, M., Ryu, Y., Sonnentag, O., Toomey, M., 2013. Climate change, phenology: and phenological control of vegetation feedbacks to the climate system. Agric. For. Meteorol. 169, 156–173.
Román, M.O., Gatebe, C.K., Schaaf, C.B., Poudyal, R., Wang, Z., King, M.D., 2011. Variability in surface BRDF at different spatial scales (30 m–500 m) over a mixed agricultural landscape as retrieved from airborne and satellite spectral measurements. Remote Sens. Environ. 115 (9), 2184–2203.
Rosenzweig, C., Casassa, G., Karoly, D.J., Imeson, A., Liu, C., Menzel, A., et al., 2007. Assessment of observed changes and responses in natural and managed systems. Clim. Change 79–131.
Ryu, Y., Lee, G., Jeon, S., Song, Y., Kimm, H., 2014. Monitoring multilayer canopy spring phenology of temperate deciduous and evergreen forests using lowcost spectral sensors. Remote Sens. Environ. 149, 227–238.
Schaber, J., Badeck, F.W., 2005. Plant phenology in Germany over the 20th century. Reg. Environ. Change 5 (1), 37–46.
Shen, M., Tang, Y., Desai, A.R., Gough, C., Chen, J., 2014. Can EVI-derived land-surface phenology be used as a surrogate for phenology of canopy photosynthesis? Int. J. Remote Sens. 35 (3), 1162–1174.
Sonnentag, O., Hufkens, K., Teshera-Sterne, C., Young, A.M., Friedl, M., Braswell, B.H., et al., 2012. Digital repeat photography for phenological research in forest

ecosystems. Agric. For. Meteorol. 152, 159–177.
Tan, B., Morisette, J.T., Wolfe, R.E., Gao, F., Ederer, G.A., Nightingale, J., Pedelty, J.A., 2008. Vegetation phenology metrics derived from temporally smoothed and gap-filled MODIS data. July. Geoscience and Remote Sensing Symposium, 2008. IGARSS 2008. IEEE International, vol. 3. pp. III-593.
Tan, B., Morisette, J.T., Wolfe, R.E., Gao, F., Ederer, G.A., Nightingale, J., Pedelty, J.A., 2011. An enhanced TIMESAT algorithm for estimating vegetation phenology metrics from MODIS data. IEEE J. Select. Top. Appl. Earth Observ. Remote Sens. 4 (2), 361–371.
USA National Phenology Network, 2015. Data from: Lilac and Honeysuckle Phenology Data 1956 – 2014. Dryad Digital Repository. http://dx.doi.org/10.5061/dryad.0262m.
Verger, A., Filella, I., Baret, F., Peñuelas, J., 2016. Vegetation baseline phenology from kilometric global LAI satellite products. Remote Sens. Environ. 178, 1–14.
Weiss, M., Baret, F., Garrigues, S., Lacaze, R., 2007. LAI and fAPAR CYCLOPES global products derived from VEGETATION. Part 2: validation and comparison with MODIS collection 4 products. Remote Sens. Environ. 110 (3), 317–331.
Westerling, A.L., Hidalgo, H.G., Cayan, D.R., Swetnam, T.W., 2006. Warming and earlier spring increase western US forest wildfire activity. Science 313 (5789), 940–943.
White, M.A., Nemani, R.R., 2003. Canopy duration has little influence on annual carbon storage in the deciduous broad leaf forest. Glob. Change Biol. 9 (7), 967–972.
White, M.A., Beurs, D., Kirsten, M., Didan, K., Inouye, D.W., Richardson, A.D., et al., 2009. Intercomparison, interpretation, and assessment of spring phenology in North America estimated from remote sensing for 1982–2006. Glob. Change Biol. 15 (10), 2335–2359.
Wu, C., Chen, J.M., 2014. Reconstruction of interannual variability of NEP using a process-based model (InTEC) with climate and atmospheric records at Fluxnet-Canada forest sites. Int. J. Climatol. 34 (5), 1715–1722.
Wu, C., Hou, X., Peng, D., Gonsamo, A., Xu, S., 2016. Land surface phenology of China's temperate ecosystems over 1999–2013: spatial–temporal patterns, interaction effects, covariation with climate and implications for productivity. Agric. For. Meteorol. 216, 177–187.
Yang, J., Pan, S., Dangal, S., Zhang, B., Wang, S., Tian, H., 2017. Continental-scale quantification of post-fire vegetation greenness recovery in temperate and boreal North America. Remote Sens. Environ. 199, 277–290.
Xiao, D., Tao, F., Liu, Y., Shi, W., Wang, M., Liu, F., et al., 2013. Observed changes in winter wheat phenology in the North China Plain for 1981–2009. Int. J. Biometeorol. 57 (2), 275–285.
Zhan, J., Deng, X., Yue, T., 2004. Landscape change detection in Yulin prefecture. J. Geogr. Sci. 14, 47–55.
Zhang, X., Friedl, M.A., Schaaf, C.B., Strahler, A.H., Hodges, J.C., Gao, F., et al., 2003. Monitoring vegetation phenology using MODIS. Remote Sens. Environ. 84 (3), 471–475.
Zhang, X., Tan, B., Yu, Y., 2014. Interannual variations and trends in global land surface phenology derived from enhanced vegetation index during 1982–2010. Int. J. Biometeorol. 58 (4), 547–564.
Zhang, X., Friedl, M.A., Schaaf, C.B., 2006. Global vegetation phenology from moderate resolution imaging spectroradiometer (MODIS): evaluation of global patterns and comparison with in situ measurements. J. Geophys. Res.: Biogeosci. 111 (G4).
Zhang, X., Tarpley, D., Sullivan, J.T., 2007. Diverse responses of vegetation phenology to a warming climate. Geophys. Res. Lett. 34 (19).
Zhang, X., 2015. Reconstruction of a complete global time series of daily vegetation index trajectory from long – term AVHRR data. Remote Sens. Environ. 156, 457–472.
Zhang, X., Wang, J., Gao, F., Liu, Y., Schaaf, C., Friedl, M., et al., 2017. Exploration of scaling effects on coarse resolution land surface phenology. Remote Sens. Environ. 190, 318–330.
Zhou, L., Tucker, C.J., Kaufmann, R.K., Slayback, D., Shabanov, N.V., Myneni, R.B., 2001. Variations in northern vegetation activity inferred from satellite data of vegetation index during 1981 to 1999. J. Geophys. Res.: Atmos. 106 (D17), 20069–20083.